

Vortex graphs as N -omers and $\mathbb{C}P^{N-1}$ Skyrmions in N -component Bose-Einstein condensates

Minoru Eto¹ and Muneto Nitta²

¹*Department of Physics, Yamagata University, Yamagata 990-8560, Japan*

²*Department of Physics, and Research and Education Center for Natural Sciences, Keio University, Hiyoshi 4-1-1, Yokohama, Kanagawa 223-8521, Japan*

(Dated: March 26, 2013)

Stable vortex N -omers are constructed in coherently coupled N -component Bose-Einstein condensates. We classify all possible N -omers in terms of the mathematical graph theory and numerically construct all graphs for $N = 2, 3, 4, 5$. We also find that N -omers are well described as $\mathbb{C}P^{N-1}$ skyrmions when inter-component and intra-component couplings are $U(N)$ symmetric, and we evaluate their size dependence on the Rabi coupling.

PACS numbers: 03.75.Lm, 03.75.Mn, 11.25.Uv, 67.85.Fg

Introduction — Exotic vortices in multi-component condensates have recently attracted considerable attention in the area of condensed matter physics; in this light, the topics of interest include exotic superconductors, superfluid ^3He , Bose-Einstein condensates (BECs), exciton-polariton condensates, and nonlinear optics. In particular, recent advances in realizing BECs in ultra-cold atomic gases have opened up new possibilities in quantum physics [1, 2]; of particular interest is the tuning of the s-wave scattering wavelength via a Feshbach resonance [3–5]. Multi-component BECs can be realized when more than one hyperfine spin state is simultaneously populated [5, 6] or when more than one species of atoms are mixed [4, 7, 8]. The recent experimental achievement of a condensate of ytterbium offers condensations up to five components [9]. Vortices in multi-component BECs have been realized experimentally [10, 11], and the structures of these vortices are considerably richer than those formed of single components [12–25]; one fascinating feature in such cases is that vortices are fractionally quantized. The study of BECs can provide an ideal opportunity to examine the dynamics of exotic vortices because these vortices can theoretically be explained via a quantitative description using the mean field theory by the Gross-Pitaevski (GP) equation and further, the vortices can be experimentally controlled to a large degree.

Vortices or fluxes are fractionally quantized in multi-gap superconductors [26–29] as in the case of multi-component BECs. One added feature of multi-gap superconductors is the presence of Josephson coupling between the gaps. Due to the presence of this coupling there appears a sine-Gordon soliton for the phase difference between the two gaps [26, 30]. When a set of two vortices in two different gaps is separated, a sine-Gordon domain wall connects the vortices, thereby resulting in a two-vortex molecule, *i.e.*, a dimer [29]. Multi-components are also present in thin-layer Josephson junctions and high- T_c superconductors with multi-layers. Recently discovered iron-based superconductors may have three gaps,

in which case there may be three-vortex molecule *i.e.*, a trimer [31]. However, the vortex molecules have not been observed directly thus far in superconductors except indirectly [32], because the repulsion between vortices is exponentially suppressed by the Meissner effect so that it cannot be balanced with the domain wall tension.

In the case of multiple hyperfine spin states of BECs, internal coherent (Rabi) couplings between multiple components can be introduced by Rabi oscillations, similar to Josephson couplings in multi-gap superconductors. As in superconductors, a sine-Gordon domain wall of the phase difference of two components appears [33]. In this light, the advantages of BECs are that Rabi coupling can be tuned experimentally and that a vortex dimer can exist stably because repulsion between two fractional vortices [20] is sufficiently strong in the absence of the Meissner effect, to be balanced with the tension of a sine-Gordon domain wall connecting them [17]. Recently, we observed stable-vortex trimers in three-component BECs, and we showed that the shape and the size of the molecule can be controlled by varying the strength of the Rabi couplings [24].

In this Letter, we construct stable-vortex N -omers, that is, molecules made of N fractional vortices in N -component BECs, and we find that N -omers with $N \geq 3$ exhibit several novel properties that dimers do not possess, *i.e.*, the existence of chirality pairs and metastable states such as twist, holding, and capture, which are properties exhibited by chemical molecules. Each condensate wave function has a nontrivial winding number around one of the N fractional vortices. When the Rabi couplings are turned on, the fractional vortices are glued by domain walls to form a vortex N -omer. We make use of the mathematical graph theory to classify the vortex N -omers whose number exponentially increases as N increases. We numerically construct all possible graphs for $N = 3, 4, 5$ by imaginary time propagation with the phase winding and a constant density fixed at the boundaries, thereby our results imply that the vortex N -omers are formed in rotating BECs. We find that two geomet-

rically different graphs topologically equivalent to each other can both be stable. Furthermore, we can control the shape and size of the molecules by varying the strength of the Rabi couplings. To demonstrate this, we construct a vortex constellation, *i. e.*, the orion. We also show that vortex N -omers are well described by $\mathbb{C}P^{N-1}$ skyrmions when all possible Rabi couplings are set to the same values, where $\mathbb{C}P^{N-1} \simeq SU(N)/[SU(N-1) \times U(1)]$ denotes the complex projective space.

N -component BECs — We consider coherently coupled N -component BECs of atoms with mass m , described by the condensate wave functions Ψ_i ($i = 1, 2, \dots, N$) with the GP energy functional

$$E = \sum_{i,j=1}^N \int d^2x \left(-\frac{\hbar^2}{2m} \Psi_i^* \nabla^2 \Psi_i \delta_{ij} + \frac{g_{ij}}{2} |\Psi_i|^2 |\Psi_j|^2 - \mu_i |\Psi_i|^2 \delta_{ij} - \omega_{ij} \Psi_i^* \Psi_j \right), \quad (1)$$

where atom-atom interactions are characterized by the coupling constants $g_{ij} = 4\pi\hbar^2 a_{ij}/m$ with s-wave scattering lengths a_{ij} , μ_i denotes the chemical potential, and $\omega_{ij} = \omega_{ji}$ ($\omega_{ii} = 0$) denotes the internal coherent coupling due to Rabi oscillations between the i -th and j -th components. We mainly consider the case where $g_{ii} \equiv g$, and $\mu_i \equiv \mu$, and $g_{ij} \equiv \tilde{g}$ ($i \neq j$) in this Letter. It is straightforward to consider the general case but all the results below are essentially unchanged from our simplest choice.

The symmetry of the Hamiltonian depends on the coupling constants g, \tilde{g} , and ω_{ij} . The maximal symmetry $U(N)$ is achieved when $g = \tilde{g}$ with $\omega_{ij} = 0$. When $g \neq \tilde{g}$ and $\omega_{ij} = 0$, this symmetry reduces to $U(1)^N$ acting on a phase of each component. When $g \neq \tilde{g}$ and $\omega_{ij} \neq 0$, it further reduces to the gauge symmetry $U(1)$ which rotates the phases of all the components uniformly.

When all the internal coherent couplings are equal *i. e.*, $\omega_{ij} = \omega$, the condensations of the ground state are $|\Psi_i| = v \equiv \sqrt{\frac{\mu + (N-1)\omega}{g + (N-1)\tilde{g}}}$, with $i = 1, 2, \dots, N$. These amplitudes are modified in the case $\omega_{ij} \neq \omega_{i'j'}$, and one should solve the variational problem $\delta E / \delta \Psi_i = 0$ to determine $v_i = |\Psi_i|$ numerically.

As long as the internal coherent couplings $|\omega_{ij}|$ are maintained sufficiently small with respect to the other couplings (we choose $g \sim \tilde{g} = \mathcal{O}(10^3)$, $\mu = \mathcal{O}(10^2)$, and $\omega = \mathcal{O}(10^{-2})$), the symmetries $U(N)$ for $g = \tilde{g}$ and $U(1)^N$ for $g \neq \tilde{g}$ are nearly intact. These symmetries are spontaneously broken in the ground state. Consequently, vortices that are quite different for $g = \tilde{g}$ and $g > \tilde{g}$ can appear. For $g = \tilde{g}$, an axisymmetric giant vortex appears. As we will explain below, this can be interpreted as a $\mathbb{C}P^{N-1}$ skyrmion. On the other hand, for $g > \tilde{g}$, there appear N fractional vortices associated with the broken $U(1)^N$ symmetry, which are connected by domain walls, thereby resulting in molecules with N

vortices.

The internal coherent couplings $-\omega_{ij} \Psi_i^* \Psi_j = -2v_i v_j \omega_{ij} \cos(\theta_i - \theta_j)$, with $\theta_i = \arg \Psi_i$, glue the fractional vortices by creating domain walls among them. For $\omega_{ij} > 0$, all the phases θ_i and θ_j coincide, *i. e.*, $\theta_i = \theta_j$ in the ground state.

First, let us consider the case that all ω_{ij} 's are zero. A vortex winding around only one component, $\Psi_i = v_i \rho(r) e^{i\theta}$, in polar coordinates r and θ , with the other components almost constant, is fractionally quantized as

$$\oint d\mathbf{r} \cdot \mathbf{v}_s = \frac{v_i^2}{\sum_i v_i^2} \frac{h}{m}, \quad (2)$$

with the superfluid velocity \mathbf{v}_s , and it is stable. However, once we turn on the internal coherent couplings ω_{ij} , no matter how tiny they are, the vortex is inevitably attached by semi-infinitely long domain walls extending to the boundary because of the Rabi energy. To examine this phenomenon, we approximate the condensate wave functions by $|\Psi_i| = v_i e^{i\theta_i}$ to obtain the reduced energy functional $\mathcal{E}_{\text{phase}} = \sum_{i=1}^N \frac{\hbar^2}{2m} (\vec{\nabla} \theta_i)^2 - 2 \sum_{i>j}^N \omega_{ij} v_i v_j \cos(\theta_i - \theta_j)$. This reduced energy functional shows that $N - 1$ domain walls are attached to the i -th vortex in the direction $\theta_i = \theta_j$. Therefore, this vortex cannot remain stable in an isolated state, and it must be connected to the boundary or to vortices winding around the other components forming the molecules.

As described below, we find that the mathematical graph theory is useful to classify the vortex molecules, where we identify vertices as vortices, and the edge connecting i -th and j -th vertices as the Rabi coupling ω_{ij} if it is nonzero.

$\mathbb{C}P^{N-1}$ skyrmions — Here, we consider the symmetric case with $g = \tilde{g}$ and with all possible internal coherent couplings being the same ($\omega_{ij} = \omega$ for all i, j), which correspond to the complete graphs. We numerically solve the GP equation by using an imaginary time propagation for $N = 3, 4, 5$, as shown in Fig. 1. We find that energy densities are always axisymmetric so that we may call them giant vortices. However, each component has a different configuration; the vortex centers of each component are expressed as dots, whose positions are \mathbb{Z}_N symmetric. We also varied ω and found that the size of the configuration decreases as ω increases, as shown in Fig. 2 for $N = 3, 4, 5$. With our numerical survey over a wide range of parameter space and various initial configurations, we conclude that the existence of vortices is robust.

We further confirm the stability and existence of the solutions by using a variational method. In the parameter region of $g \gg |\omega|$, we note from Eq. (1) that the total density is approximately constant, *i. e.*, $\sum_i |\Psi_i|^2 \simeq \mu/g$. Thus, we are naturally led to define the reduced wave functions $\{\phi_i\}$ by $\Psi_i = \sqrt{\frac{\mu}{Ng}} \phi_i$, $\sum_{i=1}^N |\phi_i|^2 = 1$. Consequently, the GP model expressed by Eq. (1) reduces to

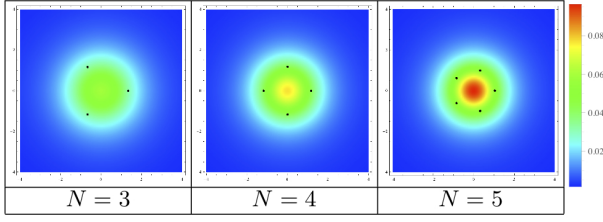


FIG. 1: Energy-density distribution of axisymmetric molecules with $m = \hbar = 1$, $g = \tilde{g} = 10^3$, $\mu = 10^2$, and $\omega = 0.05$. The size of the simulation box is $(2L)^2 = 20^2$ with the lattice space set to be less than 0.1. Zeros of Ψ_i are indicated by the black dots. The numerical range for each of the figures is set as $x \in [-4, 4]$ and $y \in [-4, 4]$.

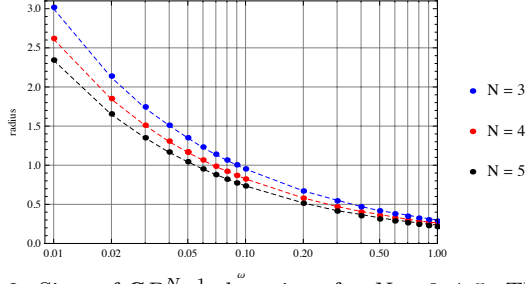


FIG. 2: Sizes of \mathbb{CP}^{N-1} skyrmions for $N = 3, 4, 5$. The dots indicate skyrmion radii obtained from the numerical solutions. The radii obtained by the variational method are connected by broken lines.

the S^{2N-1} nonlinear sigma model. Upon separating the total phase $\Theta \equiv \frac{1}{N} \sum_{i=1}^N \theta_i$, the rest of the degrees of freedom are described by the \mathbb{CP}^{N-1} model,

$$\mathcal{E}_{\mathbb{CP}^{N-1}} \simeq \frac{\mu}{Ng} \left[\frac{\hbar^2}{2m} \sum_i |\nabla \phi_i|^2 - \omega_{ij} (\phi_i^* \phi_j + \phi_i \phi_j^*) \right], \quad (3)$$

with the identification $\phi_i \sim e^{i\alpha} \phi_i$. Motivated by exact solutions of \mathbb{CP}^{N-1} skyrmions and the \mathbb{Z}_N symmetric zeros in Fig. 1, we propose a variational ansatz

$$\phi_i = \frac{z - z_i}{\sqrt{\sum_{j=1}^N |z - z_j|^2}}, \quad z \equiv x + iy, \quad (4)$$

$$z_j \equiv x_j + iy_j = \omega_N^{j-1} \lambda e^{-\frac{a}{2} r^2}, \quad \omega_N \equiv e^{\frac{2\pi i}{N}}, \quad (5)$$

with variational parameters a and λ , as a generalization of the case of $N = 2$ (\mathbb{CP}^1) [17, 18]. Substituting the above values into Eq. (3), we find

$$\begin{aligned} \frac{NgE}{2\pi\mu} &= \int_0^L dr \, r \left[\frac{\hbar^2}{2m} \frac{r^2 + \lambda^2 e^{-ar^2} + (ar^2 + 1)^2 \lambda^2 e^{-ar^2}}{(r^2 + \lambda^2 e^{-ar^2})^2} \right. \\ &\quad \left. + \omega \left(\frac{N\lambda^2 e^{-ar^2}}{r^2 + \lambda^2 e^{-ar^2}} - (N-1) \right) \right], \end{aligned} \quad (6)$$

where L denotes the system size. We next find the values of λ and a for minimizing the energy and read the size from $r = \lambda e^{-\frac{a}{2} r^2}$. In our study, we observed complete agreement between the radii obtained by the numerical solutions and the variational method, as shown in Fig. 2.

Vortex molecules — Next, let us consider the miscible case $g > \tilde{g}$ to observe non-axisymmetric configurations, namely, the vortex molecules.

Dimers: Vortex dimers are molecules of two vortices appearing in two-component BECs [17]. The dimer is the simplest molecule that does not have any degeneracies or substructures.

Trimers: Vortex trimers are molecules of three vortices appearing in three-component BECs. These exhibit two new properties that the dimers do not have. The first reported in Ref. [24] is that the shape of the triangle can be changed by tuning the parameters in Eq. (1). The second is the chirality of the triangle. This can be easily seen when the coupling constants are generic, so that the vortices have different sizes, as seen in Fig. 3. In two-component BECs, chirality does not make sense

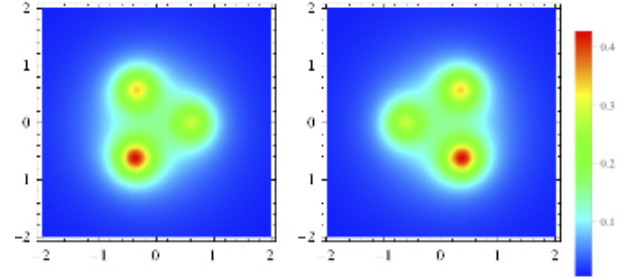


FIG. 3: Chirality: two trimers in a three-component BEC ($g_{11} \neq g_{22} \neq g_{33} \neq g_{11}$). The plotted energy densities are shown in the figures. In each figure, there are three different vortices forming a molecule. The left panel is a mirror image of the right panel.

because left and right can be exchanged by π rotation. On the other hand, as shown in Fig. 3, the left and right configurations cannot be transformed to each other by a rotation but can be transformed by a mirror. The trimers are energetically completely degenerate.

Tetramers: In multi-component BECs with more than four condensate wave functions, the number of possible molecules increases exponentially. Therefore, in order to classify such vortex molecules, we make use of the mathematical graph theory, in which vortices are expressed by vertices and the Rabi couplings are expressed by edges. Graphs isomorphic to each other are not distinguished in the graph theory. The number of independent connected graphs relevant for four-component BECs is six. In the graph theory, a graph is characterized by the sequence of the number of edges connected to each vertex. For instance, $(1, 1, 2, 2)$ implies that two vertices are connected by two edges, and other two vertices are con-

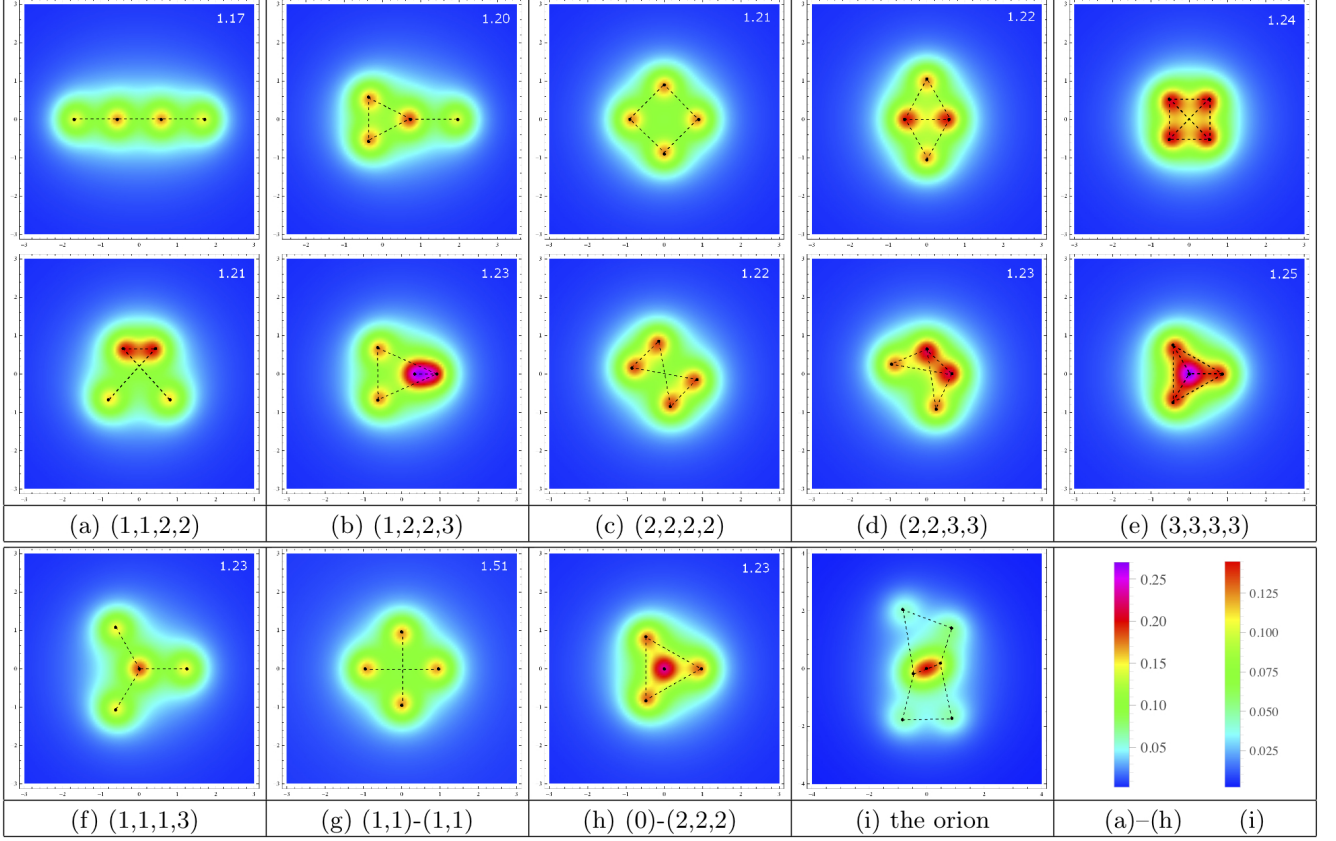


FIG. 4: (a)–(h) All possible tetramers in a four-component BEC and (i) the orion in a seven-component BEC. We set $\tilde{g} = 900$ while the other parameters are the same as those for Fig. 1. For the tetramers, we set $\omega_{ij} = 0.05$ and $\omega_{ij} = 0$ for the connected and disconnected pairs, respectively. For the orion, we set $(\omega_{12}, \omega_{23}, \omega_{34}, \omega_{45}, \omega_{16}, \omega_{56}, \omega_{37}, \omega_{67}) = (0.02, 0.001, 0.02, 0.02, 0.05, 0.02, 0.2, 0.2)$ and the rests to be zero. The dots and dotted lines indicate the vortex center of each component and the Rabi couplings between components, respectively. The color maps represent the energy density (the left for tetramers and the right for the orion). The number at the upper-right corner in each subfigure represents the total energy. As regards more precise information on the tetramers, the phase and amplitude of each component are plotted in Figs. 5 and 6, and phase differences between two among four components are plotted in Fig. 7 in the appendix. In Fig. 7, the positions of domain walls are visible.

ected by one edge. We obtained numerical solutions for a four-component BEC with the same values of Rabi couplings (Fig. 4), exhausting all possible graphs with four vortices as vertices including six connected graphs seen in Fig. 4 (a)–(f) and two disconnected graphs in Fig. 4 (g) and (h). We calculated the GP energy (1) subtracted by the ground state energy for each configuration, as shown at the top-right of each panel in Fig. 4, where we chose $r = 6$ for the spatial integration in Eq. (1).

Our simulation indicate the occurrence of several new phenomena that do not exist in dimers or trimers: 1) twist, 2) holding, and 3) capture. We have found that most molecules are accompanied by “twisted” molecules, as in Fig. 4 (a)–(e). A pair of untwisted and twisted molecules corresponds to identical graphs isomorphic to each other, while both pairs are energetically stable, corresponding to absolute and local minima; the upper configuration has lesser energy than the lower configuration

in each figure in Fig. 4 (a)–(e), and corresponds to the absolute minimum. There exists an energy barrier between twisted and untwisted molecules, and therefore, once a twisted vortex molecule is formed, a certain amount of finite energy is required to “untwist” it. As an example, a rod molecule denoted by the graph (1, 1, 2, 2) in (a) has an energy value of 1.17 when it is straight, while its energy value is 1.21 when it is twisted.

The second and third new phenomena can be observed in the disconnected graphs (g) and (h). The holding phenomenon can be observed in Fig. 4 (g). This is seen as the union of the two graphs with (1, 1). If the two domain walls connecting vortices are not crossed, this molecule breaks up into two dimers because of repulsion between the vortices. The third phenomenon observed is the absorption of a molecule inside a bigger molecule, as in Fig. 4 (h).

In the mathematical graph theory, an energy compo-

nent called the graph energy is defined motivated by the π -electron energy of molecules in chemistry [35]. In such a case, for a given graph, configurations with the minimum graph energy are unique. Our GP energy (1) provides a new definition of graph energy in the graph theory, which makes vortex molecules more interesting even mathematically.

***N*-omers:** We can engineer as many multiple vortex molecules as we want with the constituent vortices. As an example, we present vortex pentamers corresponding to all possible connected graphs with five vertices in a five-component BEC with the same Rabi couplings in Fig. 8 in the appendix.

Thus far, we have concentrated on the case when $\omega_{ij} = \omega \neq 0$ and $\omega_{ij} = 0$ for the connected and disconnected pair of the vortices, respectively. We can control the positions and shape of the molecule by varying ω_{ij} inhomogeneously. As an example, we present a vortex heptamer (seven vortices), designed as the orion in Fig. 4 (i).

Conclusion — In conclusion, we have demonstrated the construction of stable-vortex *N*-omers in coherently coupled *N*-component BECs, and we have classified all possible *N*-omers in terms of graph theory. One graph may correspond to two stable configurations which are the local and global minima. We observed several new phenomena including chirality, twist, holding, and capture. We also found that *N*-omers are well described by $\mathbb{C}P^{N-1}$ skyrmions for the $U(N)$ symmetric couplings. We used various initial conditions and always reached the same configurations (up to rotation), and therefore, we conclude that our results are consistent and verifiable. The GP energy provides a new definition of graph energy in the graph theory. When the values of ω_{ij} 's are not equal, the domain walls have tensions different from each other and the corresponding edges have weights in the graph theory. When v_i 's are not equal, the vortices have different masses and the corresponding vertices have weights.

In experiments, an integer vortex is created as usual by gradually increasing the rotation, and subsequently, it is split into a vortex *N*-omer. Two-component BECs of different hyperfine states of the same atom have been already realized using the $|1, -1\rangle$ and $|2, 1\rangle$ states [10] and the $|2, 1\rangle$ and $|2, 2\rangle$ states [34] of ^{87}Rb , respectively. We believe that systems with three or more components can be realized by using a mixture of the above mentioned states of ^{87}Rb via an optical trap [36], and our prediction is testable in laboratory experiments.

This work is supported in part by KAKENHI (No. 23740198, No. 23740226, and No. 23103515)

-
- [1] C. J. Pethick and H. Smith, *Bose-Einstein Condensation in Dilute Gases*, 2nd ed. (Cambridge University Press, New York, 2008).
 - [2] M. Ueda, *Fundamental and New Frontiers of Bose-Einstein Condensation*, (World Scientific, 2010).
 - [3] G. Thalhammer, G. Barontini, L. De Sarlo, J. Catani, F. Minardi, and M. Inguscio, Phys. Rev. Lett. **100**, 210402 (2008).
 - [4] S. B. Papp, J. M. Pino, and C. E. Wieman, Phys. Rev. Lett. **101**, 040402 (2008).
 - [5] S. Tojo, Y. Taguchi, Y. Masuyama, T. Hayashi, H. Saito, and T. Hirano, Phys. Rev. A **82**, 033609 (2010).
 - [6] C. J. Myatt, E. A. Burt, R. W. Ghrist, E. A. Cornell, and C. E. Wieman, Phys. Rev. Lett. **78**, 586 (1997); D. S. Hall, M. R. Matthews, J. R. Ensher, C. E. Wieman, and E. A. Cornell, Phys. Rev. Lett. **81**, 1539 (1998); M. Mertes, J. W. Merrill, R. Carretero-González, D. J. Frantzeskakis, P. G. Kevrekidis, and D. S. Hall, Phys. Rev. Lett. **99**, 190402 (2007).
 - [7] G. Modugno, M. Modugno, F. Riboli, G. Roati, and M. Inguscio, Phys. Rev. Lett. **89**, 190404 (2002); G. Thalhammer, G. Barontini, L. De Sarlo, J. Catani, F. Minardi, and M. Inguscio, Phys. Rev. Lett. **100**, 210402 (2008).
 - [8] D. J. McCarron, H. W. Cho, D. L. Jenkin, M. P. Köppinger, and S. L. Cornish, Phys. Rev. A **84**, 011603(R) (2011).
 - [9] T. Fukuhara, S. Sugawa and Y. Takahashi, Phys. Rev. A **76**, 051604(R) (2007).
 - [10] M. R. Matthews, B. P. Anderson, P. C. Haljan, D. S. Hall, C. E. Wieman, and E. A. Cornell, Phys. Rev. Lett. **83**, 2498 (1999).
 - [11] V. Schweikhard, I. Coddington, P. Engels, S. Tung, and E. A. Cornell Phys. Rev. Lett. **93**, 210403 (2004).
 - [12] T.-L. Ho, Phys. Rev. Lett. **81**, 742-745 (1998); T. Ohmi and K. Machida, J. Phys. Soc. Jpn. **67**, 1822 (1998).
 - [13] G. W. Semenoff and F. Zhou, Phys. Rev. Lett. **98** (2007) 100401; M. Kobayashi, Y. Kawaguchi, M. Nitta and M. Ueda, Phys. Rev. Lett. **103** (2009) 115301.
 - [14] A. M. Turner and E. Demler, Phys. Rev. B **79**, 214522 (2009).
 - [15] E. J. Mueller and T.-L. Ho, Phys. Rev. Lett. **88**, 180403 (2002).
 - [16] K. Kasamatsu, M. Tsubota and M. Ueda, Phys. Rev. Lett. **91**, 150406 (2003).
 - [17] K. Kasamatsu, M. Tsubota and M. Ueda, Phys. Rev. Lett. **93**, 250406 (2004).
 - [18] K. Kasamatsu, M. Tsubota and M. Ueda, Int. J. Mod. Phys. B **19**, 1835 (2005).
 - [19] K. Kasamatsu, and M. Tsubota, Phys. Rev. A **79**, 023606 (2009).
 - [20] M. Eto, K. Kasamatsu, M. Nitta, H. Takeuchi and M. Tsubota, Phys. Rev. A **83**, 063603 (2011).
 - [21] P. Mason and A. Aftalion, Phys. Rev. A **84**, 033611 (2011).
 - [22] A. Aftalion, P. Mason and W. Juncheng, Phys. Rev. A **85**, 033614 (2012).
 - [23] P. Kuopanportti, J. A. M. Huhtamäki, M. Möttönen, Phys. Rev. A **85**, 043613 (2012).
 - [24] M. Eto and M. Nitta, Phys. Rev. A **85**, 053645 (2012).
 - [25] M. Cipriani and M. Nitta, arXiv:1303.2592 [cond-

- mat.quant-gas].
- [26] Y. Tanaka, J. Phys. Soc. Jp. **70**, 2844 (2001); Phys. Rev. Lett. **88**, 017002 (2001).
 - [27] E. Babaev, Phys. Rev. Lett. **89** (2002) 067001; E. Babaev, A. Sudbo and N. W. Ashcroft, Nature **431**, 666 (2004); J. Smiseth, E. Smorgrav, E. Babaev and A. Sudbo, Phys. Rev. B **71**, 214509 (2005); E. Babaev and N. W. Ashcroft, Nature Phys. **3**, 530 (2007).
 - [28] A. Gurevich and V. M. Vinokur, Phys. Rev. Lett. **90**, 047004 (2003).
 - [29] J. Goryo, S. Soma and H. Matsukawa, Euro Phys. Lett. **80**, 17002 (2007).
 - [30] H. Bluhm, N. C. Koshnick, M. E. Huber, and K. A. Moler, Phys. Rev. Lett. **97**, 237002 (2006).
 - [31] M. Nitta, M. Eto, T. Fujimori and K. Ohashi, J. Phys. Soc. Jap. **81**, 084711 (2012).
 - [32] A. Crisan *et.al*, Jpn. J. Appl. Phys. **46**, L451-L453 (2007); Y. Tanaka *et.al*, Jpn. J. Appl. Phys. **46**, 134-145 (2007); A. Crisan *et.al*, Phys. Rev. **B** 77, 144518 (2008); J. W. Guikema *et.al*, Phys. Rev. **B** 77, 104515 (2008); L. Luan *et.al*, Phys. Rev. **B** 79, 214530 (2009).
 - [33] D. T. Son, M. A. Stephanov, Phys. Rev. A **65**, 063621 (2002).
 - [34] P. Maddaloni, M. Modugno, C. Fort, F. Minardi, and M. Inguscio, Phys. Rev. Lett. **85**, 2413 (2000).
 - [35] I. Gutman, O. E. Polansky, *Mathematical Concepts in Organic Chemistry*, (Springer-Verlag, Berlin 1986); I. Gutman, J. Serb. Chem. Soc. 70 (3) 441456 (2005).
 - [36] C. Hamner, J. J. Chang, P. Engels, and M. A. Hoefer, Phys. Rev. Lett. **106**, 065302 (2011).

Appendix — Here, we provide more detailed information on our numerical solutions. Figures 5 and 6, show the plots of the amplitudes and the phases of condensate wave functions Ψ_i for the tetramers shown in Figs. 4(a)-(h). We also show the relative phases of Ψ_i in Fig. 7. The figures clearly indicate that the condition $\theta_i = \theta_j$ at the boundary is satisfied along with showing the positions of the sine-Gordon domain walls.

Finally, we illustrate in Fig. 8 all the vortex pentamers in a five component BEC that are topologically inequivalent.

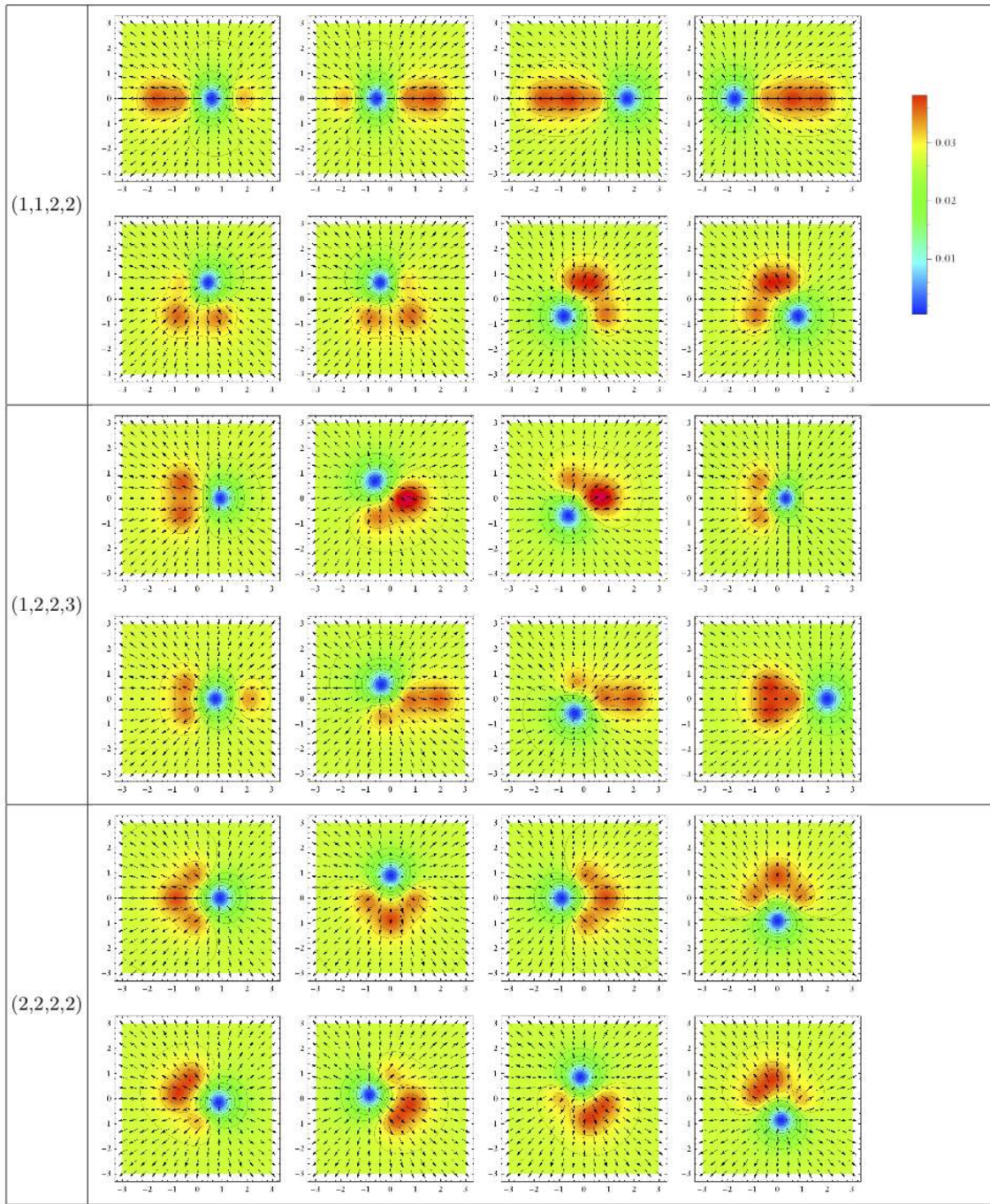


FIG. 5: The amplitudes and phases of Ψ_1, Ψ_2, Ψ_3 , and Ψ_4 for the tetramers shown in Fig. 4. The arrows indicate the phase vector ($\text{Re}\Psi_i, \text{Im}\Psi_i$). The colors indicate the amplitudes of the condensate wave functions.

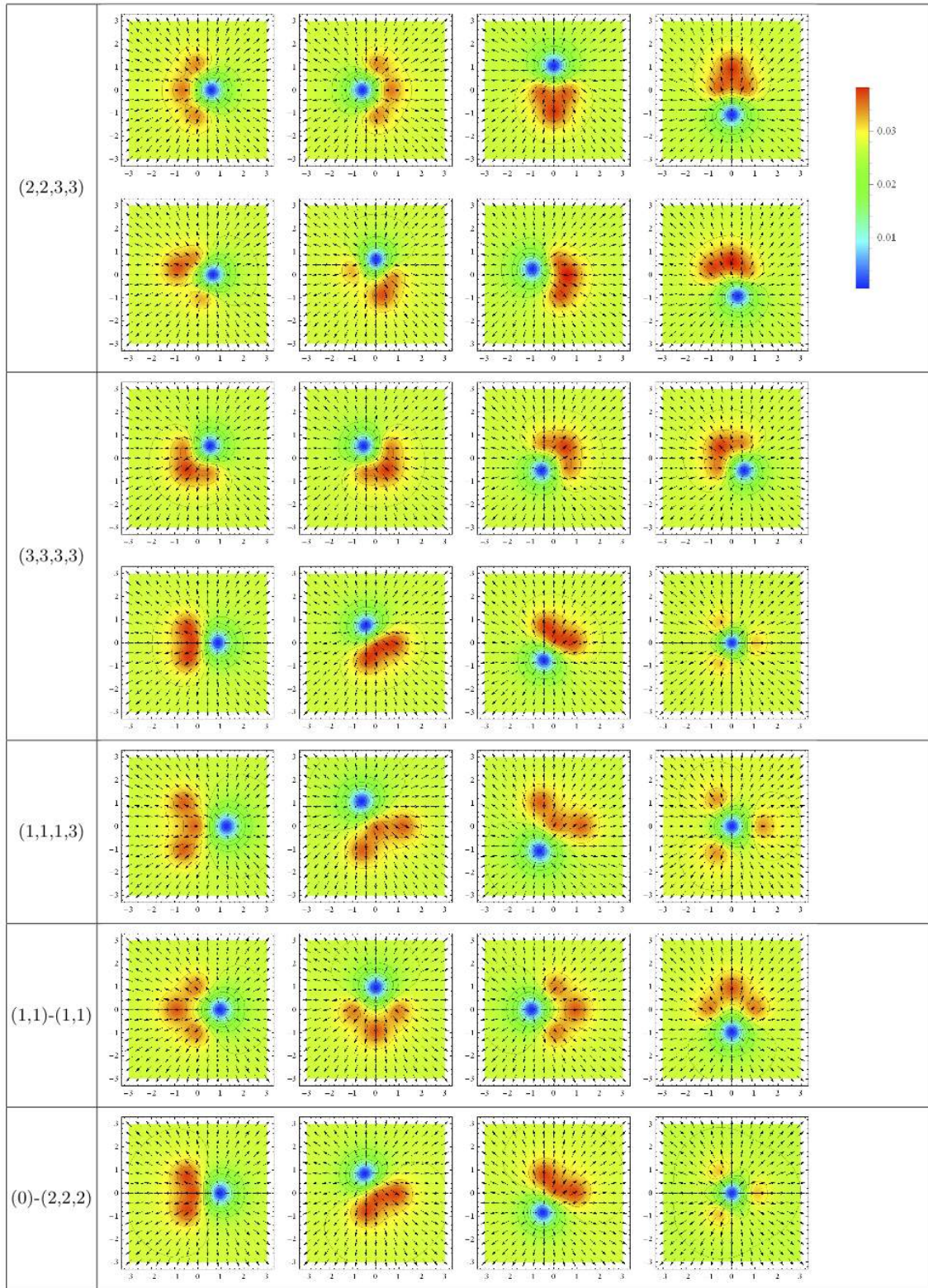


FIG. 6: See the caption of Fig. 5.

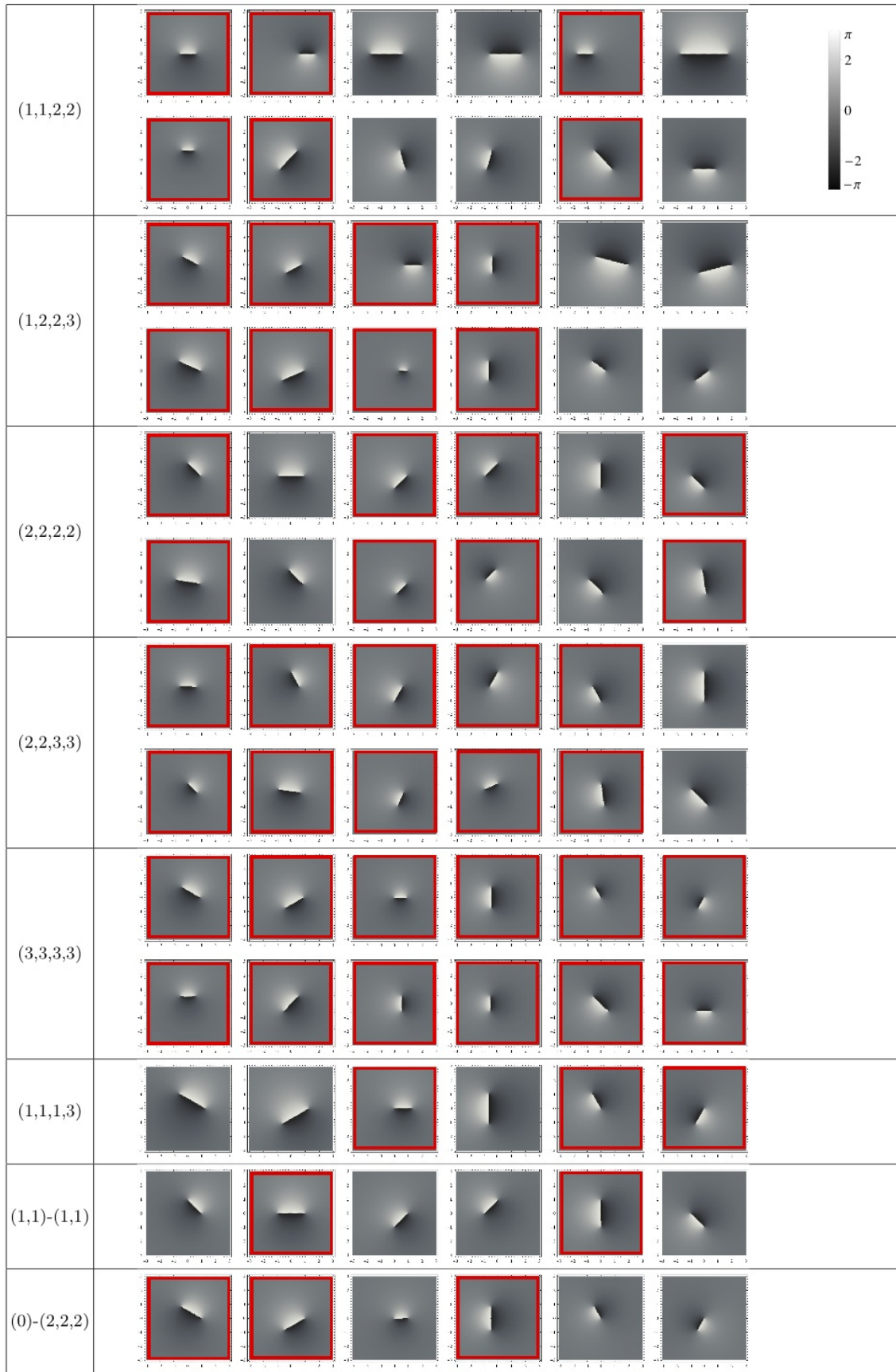


FIG. 7: The relative phases ($\arg \Psi_i - \arg \Psi_j$ for $\{i, j\} = \{(1, 2), (1, 3), (1, 4), (2, 3), (2, 4), (3, 4)\}$) for the tetramers shown in Fig. 4. The panels surrounded by the red squares correspond to the relative phases for the non-zero Rabi frequencies. Namely, they show the positions of the sine-Gordon domain walls.

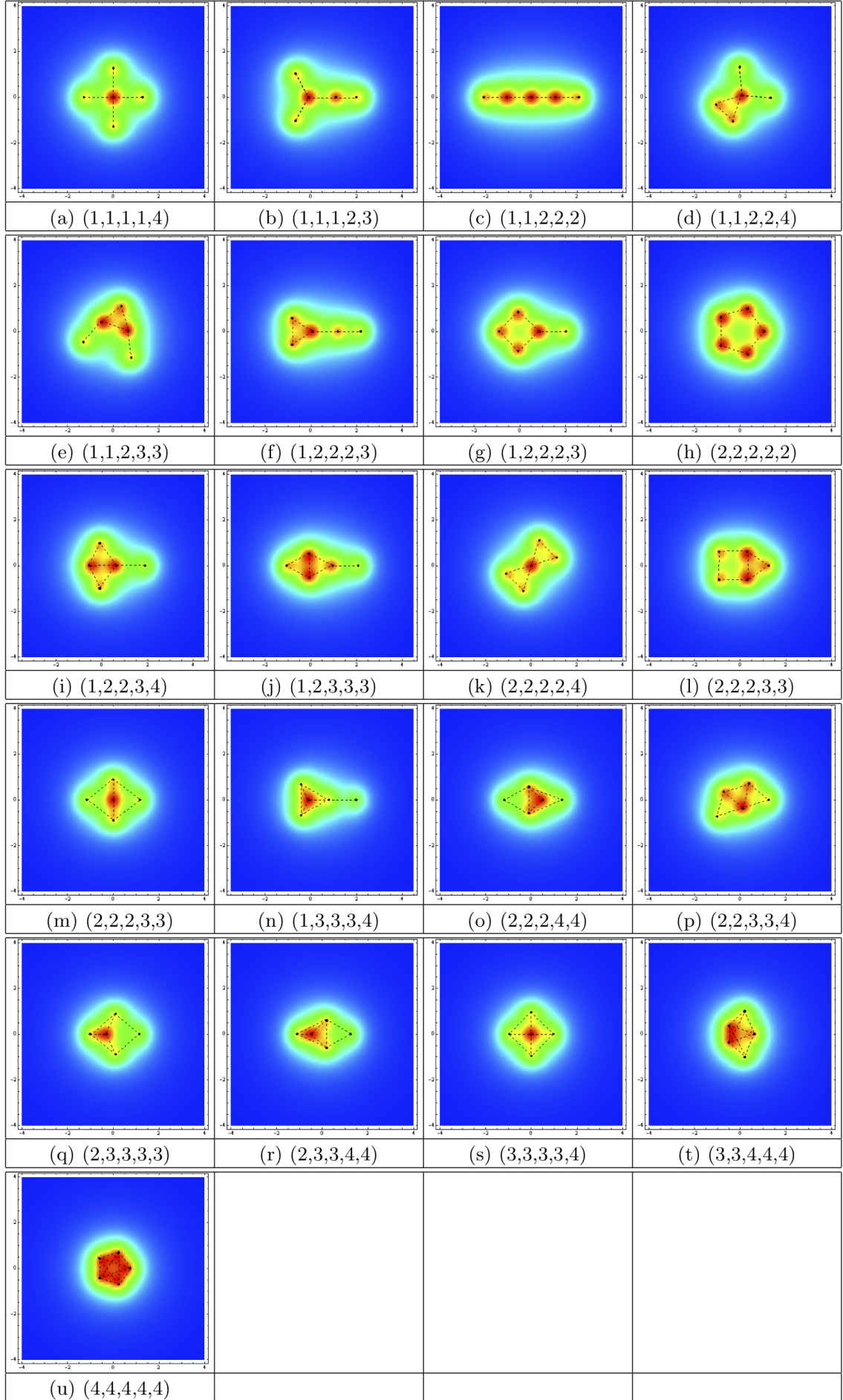


FIG. 8: Representatives of all connected pentamers with the least energy in a five component BEC. All parameters are the same as those in Fig. 4.